Proceedings of the 1998 IEEE/RSJ
Intl. Conference on Intelligent Robots and Systems
Victoria, B.C., Canada • October 1998

Exploring Spherical Image Properties for Robot Navigation

Inácio Fonseca
Institute of Systems and Robotics,
Electrical Engineering Department,
Polo II, University of Coimbra,
3030 COIMBRA, Portugal,
sousa@isr.uc.pt
Fax: +351-39-406672

Jorge Dias
Institute of Systems and Robotics,
Electrical Engineering Department,
Polo II, University of Coimbra,
3030 COIMBRA, Portugal,
jorge@isr.uc.pt
Fax: +351-39-406672

Abstract

This paper addresses the problem of performing navigation with a mobile robot using active vision exploring the image sphere properties in a stereo divergent configuration. The navigational process is supported by the control of the robot's steering and forward movements just using visual information as feedback. The steering control solution is based on the difference between signals of visual motion flow computed in images on different positions of a virtual image sphere. The majority of solutions based on motion flow and proposed until now, where usually very unstable because they normally compute other parameters from the motion flow. In our case the control is based directly on the difference between motion flow signals on different images. Those multiple images are obtained by small mirrors, that simulates cameras positioned in different positions on the image sphere. At this moment it is under development another new version for the spherical sensor. The control algorithm described in this work is based on discrete-event approach to generate a controlling feedback signal for navigation of an autonomous robot with an active vision system as described on [2].

1 Introduction

In this article we propose an algorithm based on visual information to drive a mobile robot indoors. Several solutions have been proposed by different authors (see [6], [7], [4] and [3] for some examples), but we propose a different solution, based on image sphere. The goal for the final prototype is to run the system without any collision against static and mobile obstacles. In this prototype we built part of the sphere using mirrors. The approach uses two cameras, that have been mounted with mirrors to simulate more than two points of view in a total of two images by each camera. From these two images and from the optical flow measurements, a signal proportional to the orientation between the wall and the mobile robot can be obtained for each side. The next section describes in detail this approach, and for a better understanding of this study, we will introduce the concept of image sphere for visual based navigation. It is also explained how we simulate this sphere partially, using mirrors and cameras. For the study we assume the image sphere centered in the robot's locomotion referential. The idea is to study the best cameras' positions in the spherical sensor surface to achieve the best results for different tasks. However, first we will study the problem as if we have a real spherical sensor, and finally it will be described the differences when real cameras are used.

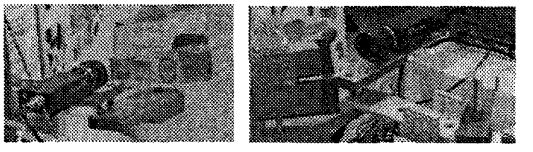

Figure 1: The mobile system with the mirror setup to simulate four points of view.

2 Mathematical Background

2.1 The spherical sensor

Suppose that we want to control the attitude of a three-dimensional vehicle in the space, while the system is moving. Considering the referential system represented in the Fig. 2 and modeling the visual sensor as a spherical sensor with a radius r, we only need to

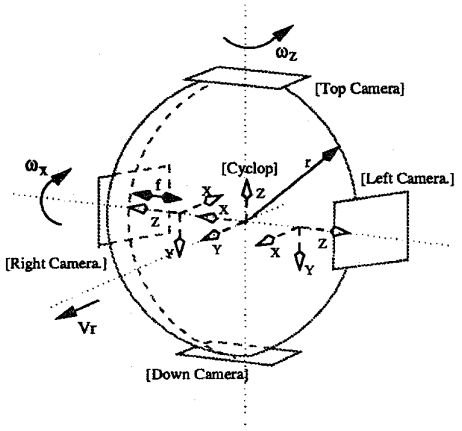

Figure 2: The sphere model for the navigation system in a three dimensional world.

control the three velocities indicated in the figure (not considering the swing degree of freedom).

The first problem is how to determine the minimal number of cameras to use and where to put them in the spherical surface to estimate the necessary information to control the vehicle. Bergholm [1] argues that the flow measured in the spherical equator perpendicular to the direction of translation, gives an estimation about the depth. So, to analyze the self projected flow in the spherical surface by convenience, we will set $r = 1$. The sphere's velocity can be described as $(\vec{v}, \vec{\omega})$ with $\vec{v}$,$\vec{\omega} \in R^3$. Let d be the distance from the sphere center to a three-dimensional point X with a vector $\vec{x}$ (the depth of the viewed point). Then $d = \sqrt{x^2 + y^2 + z^2}$ and the following relation is valid:

$$\dot{\vec{x}} = \vec{\omega} \wedge \vec{x} + (\vec{v}/d). \parallel \vec{x} \parallel \quad (1)$$

It is also true, that any point P belonging to the X projection line can be described as $\vec{p} = \mu.\vec{x}, \mu > 0$, and in particular if P belongs to the sphere surface then $\parallel \vec{p} \parallel = 1$. The X velocity projected in the sphere point P is then given by:

$$\dot{\vec{p}} = \vec{\omega} \wedge \vec{p} + (\vec{v}/d) \quad (2)$$

This velocity vector can be decomposed in any orthogonal referential, and in particular our choice will be the left referential represented in Fig. 3 by $[\vec{e}_x, \vec{e}_y, \vec{e}_z]$, because with this choice we can study the flow in the equator and in the direction normal to the equator. The point P described in referential $[\vec{e}_x, \vec{e}_y, \vec{e}_z]$ has coordinates $[\cos(\theta), \sin(\theta), 0]$, the vectors are given by $\vec{e}_y = [-\sin(\theta), \cos(\theta), 0]$, $\vec{e}_z = [0, 0, 1]$, and the $\vec{e}_x$ is not important because

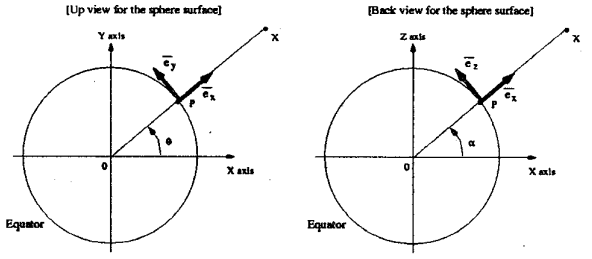

Figure 3: Decomposition of $\dot{\vec{p}}$ velocity in the referential described by the vectors $[\vec{e}_x, \vec{e}_y, \vec{e}_z]$.

we cannot measure this flow in the sphere surface. In this case we will have:

$$\begin{cases} \vec{e}_y.\dot{\vec{p}} = \omega_z + \cos(\theta).v_y/d - \sin(\theta).v_x/d \\ \vec{e}_z.\dot{\vec{p}} = \omega_x.\sin(\theta) - \omega_y.\cos(\theta) + v_z/d \end{cases} \quad (3)$$

However, in our case the sphere velocities are given by $\vec{v} = [0, v_y, 0]$ or $\vec{v} = [0, v_r, 0]$ and $\vec{\omega} = [\omega_x, 0, \omega_z]$ so the equation (3) can be reduce to:

$$\begin{cases} \vec{e}_y.\dot{\vec{p}} = \omega_z + \cos(\theta).v_y/d \\ \vec{e}_z.\dot{\vec{p}} = \omega_x.\sin(\theta) \end{cases} \quad (4)$$

That is, with the equator normal flow $\vec{e}_z.\dot{\vec{p}}$ we can estimate the ω_x velocity because it not depends from depth d. The equator parallel flow $\vec{e}_y.\dot{\vec{p}}$ depends from ω_z but using the difference between the optical flow sensed in two points it is possible to remove it.

Similarly for the plane $y = 0$ after doing the same analysis for the equator normal flow now $\vec{e}_y.\dot{\vec{p}}$ and equator parallel flow now $\vec{e}_z.\dot{\vec{p}}$ (now using the right referential in Fig. 3 by $[\vec{e}_x, \vec{e}_y, \vec{e}_z]$):

$$\begin{cases} \vec{e}_y.\dot{\vec{p}} = \omega_z.\cos(\alpha) - \omega_x.\sin(\alpha) + v_y/d \\ \vec{e}_z.\dot{\vec{p}} = 0 \end{cases} \quad (5)$$

After this study, the question is how can we control the system using the velocity measured in the sphere? We must compare the depth between two (or more) three dimensional points because the idea is to control the ω_z and ω_x velocities, then in this case we need to compare divergent points in the sphere.

For simplicity let's first consider the ω_z control. From the Fig 4, we have for the first case with divergent points, where the flow $\vec{e}_y.\dot{\vec{p}}$ is used (equation (4)),

- $\vec{e}_y.\dot{\vec{p}}_2 + \vec{e}_y.\dot{\vec{p}}_1 = 2\omega_z + v_y\left(\frac{1}{d_2} - \frac{1}{d_1}\right)$ that depends from ω_z
- $\vec{e}_y.\dot{\vec{p}}_2 - \vec{e}_y.\dot{\vec{p}}_1 = v_y\left(\frac{1}{d_1} + \frac{1}{d_2}\right)$ and we cannot compute the depth between the two points

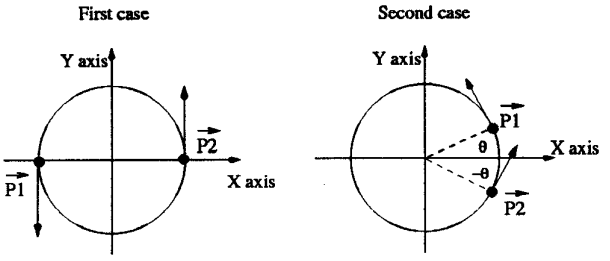

Figure 4: Representation of the relevant points to control the ω_z velocity.

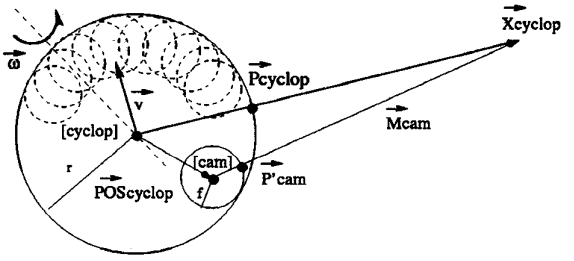

Figure 5: Patches from the spherical sensor given by small spherical sensors that are tangent to the imaginary sphere with radius r.

For the second case from the same figure using two points of view from the same lateral position, where the flow $\vec{e}_y.\dot{\vec{p}}$ is used (equation (4)),

- $\vec{e}_y.\dot{\vec{p}}_2 + \vec{e}_y.\dot{\vec{p}}_1 = 2\omega_z + \cos(\theta)v_y\left(\frac{1}{d_2} + \frac{1}{d_1}\right)$ - that depends from ω_z
- $\vec{e}_y.\dot{\vec{p}}_2 - \vec{e}_y.\dot{\vec{p}}_1 = \cos(\theta)v_y\left(\frac{1}{d_2} - \frac{1}{d_1}\right)$, it is possible to compare the depth between both points in presence of rotational movements ω_z and ω_x

From this analysis, the conclusion is that to control the ω_z velocity we must use four cameras, two for each lateral side. The control is also done in an independent way, i.e., we have a measure proportional to the orientation of each wall with the locomotion referential.

For the control of ω_x we only need two cameras pointing as represented in Fig 2 by [*TopCamera*] and [*DownCamera*], because the ω_x value can be estimated by the flow given in the lateral cameras as explained earlier. So in this case using the equator normal flow $\vec{e}_y.\dot{\vec{p}}$ from equation (5), the difference between the flow in the top and in the down side of the sphere is given by:

$$-2\omega_x + v_y\left(\frac{1}{d_2} - \frac{1}{d_1}\right) \tag{6}$$

where ω_x can be removed by using the estimation given by the equator normal flow $\vec{e}_z.\dot{\vec{p}}$ of the equation (4).

Notice that if we chose to measure the feedback signal only when the mobile robot is moving with linear velocity, the system only needs to have the four cameras and the best positions are those represented in the Fig. 2. With the left and right cameras the system can sense and control the ω_z velocity and with the others two the ω_x velocity. However with only four cameras it is impossible to control the system while doing angular movements, and to solve this problem it will be used two points of view for each lateral camera as explained earlier.

2.2 Patches from the spherical sensor given by small spherical sensors

However, it is not possible to be sure that the spherical sensor is aligned with the locomotion referential. To analyse this, suppose a small displacement of the image sphere.

The small spherical sensor with radius f represented in Fig. 5 gives patches from the original spherical sensor with radius r, that is now an imaginary sensor. We want to compare the differences between the measures done in both spheres for the same three dimensional point. The velocity in the imaginary sphere is given by

$$\dot{\vec{p}}_{cyclop} = \vec{\omega} \wedge \frac{\vec{x}_{cyclop}}{\| \vec{x}_{cyclop} \|} r + \frac{\vec{v}}{\| \vec{x}_{cyclop} \|} r \tag{7}$$

For the small sphere the following relations are true:

$$\begin{cases} \vec{M}_{cyclop} = \vec{P}os_{cyclop} + {}^{cyclop}R_{cam}\vec{M}_{cam} = \vec{x}_{cyclop} \\ \| \vec{M}_{cam} \| = \| \vec{x}_{cyclop} - \vec{P}os_{cyclop} \| \end{cases} \tag{8}$$

where ${}^{cyclop}R_{cam}$ represents the rotation matrix between the referentials associated with the spheres. In this case the velocity in the small sphere is:

$$\dot{\vec{p}}'_{cam} = \left[{}^{cyclop}R_{cam}\right]^{-1} \frac{\vec{\omega} \wedge \vec{x}_{cyclop} + \vec{v}}{\| \vec{M}_{cam} \|} f \tag{9}$$

but expressing this velocity in the [cyclop], we will get:

$$\dot{\vec{p}}'_{cyclop} = \dot{\vec{p}}_{cyclop} \frac{\| \vec{x}_{cyclop} \|}{\| \vec{x}_{cyclop} - \vec{P}os_{cyclop} \|} \frac{f}{r} \tag{10}$$

Comparing equations (7) and (10), the differences are in the factor $\frac{f}{r}$ that we know and the unknown $G =$

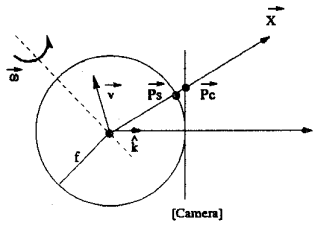

Figure 6: Differences between a spherical sensor and a conventional camera with the geometrical projection model.

$\frac{\|\vec{x}_{cyclop}\|}{\|\vec{x}_{cyclop}-\vec{Pos}_{cyclop}\|}$ that is the ratio between the depth measured in the big sphere and the depth measured at the small sphere.

For example if $r = 15cm$, $f = 25mm$ and $\| \vec{x}_{cyclop} \| >> 1,5m$ this factor will be $G \approx 1,091$ and in the presence of lower velocities it will be negligible.

2.3 Image sphere simulation by small off-the-shelf cameras

In a practical setup, we use off-the-shelf cameras with a geometrical model, so it is important to study the differences between the use of a camera and a small spherical sensor.

Considering the setup in Fig. 6, the $\vec{x}$ velocity in the sphere point $\vec{p}_s$ is $\dot{\vec{p}}_s = \frac{\dot{\vec{x}}}{\|\vec{x}\|} f$, but we can only measure in the sphere's surface the velocity $\dot{\vec{p}}_s = \frac{\dot{\vec{x}}}{\|\vec{x}\|} f - \frac{\dot{\vec{x}}.\vec{x}}{\|\vec{x}\|} f \frac{\vec{x}}{\|\vec{x}\|}$. For the camera, differentiating the geometrical projection law $\vec{p}_c = \frac{f}{\vec{x}.\hat{k}}\vec{x}$ in order of t, we can express $\dot{\vec{p}}_c = \frac{f}{\vec{x}.\hat{k}}\dot{\vec{x}} - \frac{f}{(\vec{x}.\hat{k})^2}\left(\dot{\vec{x}}.\hat{k}\right)\vec{x}$, and using the $\vec{x}$ velocity in this expression, we will get the final result that unfortunately is not equal to the measured velocity in the sphere's surface. However if the $\vec{x}$ vector points in the $\hat{k}$ direction the two velocities are actually the same. So in conclusion, we can only use the portion of the digital image that is tangent with the spherical surface, because just at this position the measured velocities will be very similar.

3 Control Algorithm and Results

3.1 Control Algorithm

In this section it will be described an experimental system used to test the approach presented in this article. The system, described on [2], uses a navigation controller based on the signals obtained by processing two images. The control system was designed

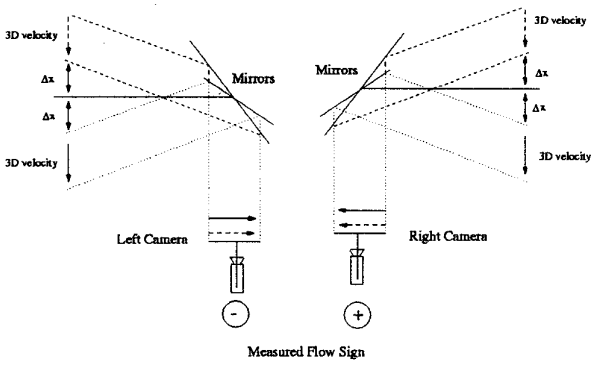

Figure 7: The mirror setup. In this case for simplicity the cameras do not have been represented as a geometrical model.

by using Discrete-Event-Systems (DES) approach. In this experimental system the mirrors are positioned in a stereo divergent way, acquiring images in the big circle of the image sphere (equator). Using the two signals from the both walls, it will be possible to estimate the wall orientation. The signal measured in each image is the horizontal optical flow or as wish the horizontal displacement, that can be given by any one-dimensional optical flow or a correlation technique. In our case the both are used to give a strong validation for the measure. The mirror setup is represented in Fig. 7.

Considering the signals measured in the mirrors by:

- **FRMM** - Front Right Mirror Measure, optical flow measured in the front right image
- **BRMM** - Back Right Mirror Measure, optical flow measured in the back right image
- **FLMM** - Front Right Mirror Measure, optical flow measured in the front left image
- **BLMM** - Back Right Mirror Measure, optical flow measured in the back left image

the control strategy can be described as (just considering the right side):

- if $\| FRMM - BRMM \| < threshold$ then the robot can rotate to the left or do translations,
- if $FRMM - BRMM > threshold$ then the robot must rotate to the left,
- if $FRMM - BRMM < threshold$ then the robot can rotate to the left/right or going to the front (depends from the measures in the left side),

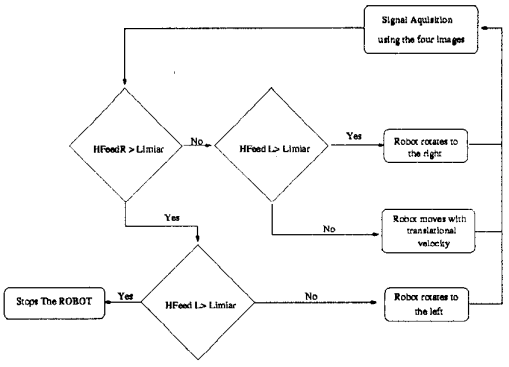

Figure 8: The control Algorithm diagram.

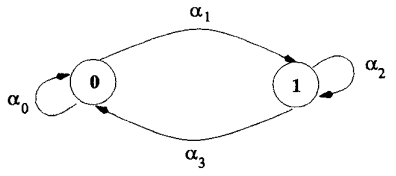

$\Sigma_u = \{ \alpha_0, \alpha_1, \alpha_2, \alpha_3 \}$

State Description

0: Acquisition
1: Control

Event Description

α_0: wait until the next control timing arrives, i.e., 0,5s doing measures
α_1: acquisition finished
α_2: control update not yet finished
α_3: command sent successful for the robot

Figure 9: The Discrete Event System definition.

Defining $HfeedR = FRMM - BRMM$ and $HfeedL = FLMM - BLMM$ the algorithm including both sides can be described by the diagram represented in Fig. 8. In this case the forward velocity is constant and the system only controls the angular velocity. The acquisition loop timing is different from the control loop timing, in this case respectively $0,08$ seconds and $0,5$ seconds. To help the control and acquisition timings we use a DES (Discrete Event System) to monitor the algorithm presented in Fig. 8. When the system is rotating, the measured signals are dropped out. One of the states is responsible to monitor the acquisition and the other to monitor the communications with the mobile robot. Because the timings involved are different the final measure for each image is the mean in the acquisition interval.

Figure 10: The result for the navigation with mirrors (external images).

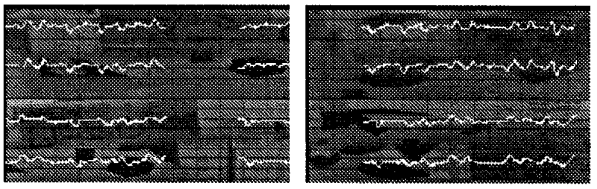

Figure 11: The result for the navigation with mirrors (internal images).

3.2 Experimental Results

The Figs. 10 and 11 show the experimental results for the navigation process with mirrors and Fig 12, 13 show the measured signals to control the mobile platform.

4 Conclusions

The paper addressed the problem of visual based navigation, using a mobile robot. The vision system realizes partially the concept of image sphere by using a stereo divergent system. To obtain more than two images in the sphere, mirrors were used. In the paper we presented an algorithm for navigation control based

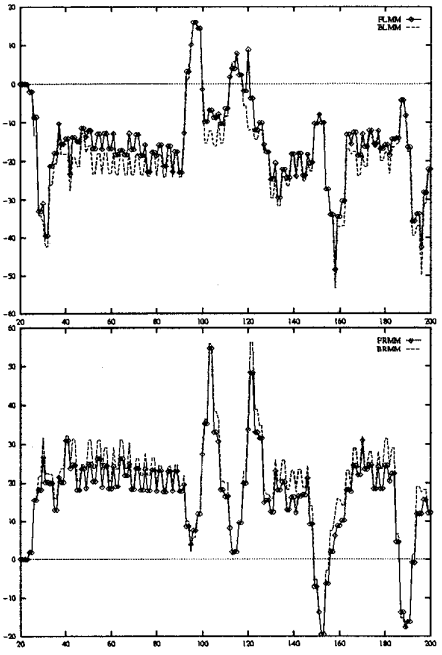

Figure 12: Measures for the signals $FLMM/BLMM$ and $FRMM/BLMM$ respectively. Time of acquisition or time unit is 0,08 seconds or 12,5Hz.

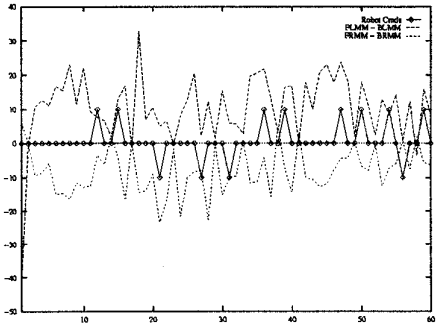

Figure 13: Feedback measures versus the commands sent to the mobile platform for the example showed in Fig 11, 12,13. Time unit: 0,5 seconds. Commands: 0 - Forward movement, -10 - Right movement, 10 - Left movement.

on the difference between the image flow on different positions of image sphere.

4.1 Acknowledgments

This work was sponsored by PO-ROBOT project from NATO Science for Stability program, and by JNICT on the framework of the SIRMA project.

References

[1] F. Bergholm,"Decomposition Theory and Transformations of Visual Directions", *ICCV 90- Int. Conf. on Computer Vision*, Dec 1990, pp. 85-90.

[2] Jorge Dias, Carlos Paredes, Inácio Fonseca, Jorge Batista, Helder Araújo, A.de Almeida, " Simulating Pursuit with Machines, Using Active Vision and Mobile Robots", *IEEE Transactions on Robotics and Automation*, February 1998, Volume 14, Number 1, pp 1-18.

[3] J. Santos-Victor, G.Sandini, F.Curotto, S.Garibaldi, *Divergent Stereo in Autonomous Navigation: From Bees to Robots* VisLab-TR 01/95, International Journal of Computer Vision, 14, pp 159-177, March 1995.

[4] Nelson, R.C., Aloimonos, J., *Finding Motion Parameters From Spherical Flow Fields (Or The Advantages Of Having Eyes In The Back Of Your Head)*, WCV(87), pp. 145-150.

[5] Roger, A. S. and Schwartz, E.L. "Design considerations for a Space-Variant Sensor with Complex Logarithmic Geometry", *Proc. 10th International Conference on Pattern Recognition*,Atlantic City, pp. 278-285,1990.

[6] Alberto Elfes, " Robot Navigation: Integrating Perception, Environmental Constraints and Task Execution Within a Probabilistic Framework", *International Workshop, Ressoning with Uncertainty in Robotics Conf. - RUR*, 95, Amsterdam, The Netherlands, December 1995, Springer ISBN 3-540-61376-5.Proc.

[7] Andrew J Davison and David W Murray, "Mobile Robot Localisation Using Active Vision", Parks Road, Oxford University, 1997.